Development of Polyphthalocyanine Based Electrocatalysts for Electrochemical CO_2 Reduction

Prof. Huabin Zhang

Under the mentorship Ph.D student

Abdulrahman Allangawi

abdulrahman.allangawi@kaust.edu.sa

Rana Mutlaq Alzahrani

Rana.alzahrani@kaust.edu.sa

Abstract

Electrochemical CO_2 reduction reaction (CO_2RR) offers a promising approach for converting CO_2 into value added chemicals and fuels using renewable electricity. Metal polyphthalocyanines (MPPc) provide well defined metal-N_4 active sites and extended π-conjugated structures, making them attractive platforms for investigating the relationship between metal composition, electronic structure, and CO_2RR performance. In this work, MnPPc and bimetallic Co_5Mn_1PPc were synthesized by a solid phase method and systematically evaluated for their structural and electrochemical properties. XRD, FTIR, and SEM characterization confirmed the formation of polyphthalocyanine-based materials and revealed differences in crystallinity and morphology following Co incorporation. Electrochemical measurements in an H-type cell using 0.5 M $KHCO_3$ demonstrated a clear difference in catalytic behavior between the two materials. MnPPc predominantly favored the hydrogen evolution reaction, with H_2 as the major product and limited CO formation. In contrast, Co_5Mn_1PPc exhibited substantially higher and more stable current densities and significantly improved CO_2RR selectivity, achieving FE_{CO} values of approximately 70–90%. Methanol was also detected at more negative potentials, indicating the potential of Co_5Mn_1PPc to promote further reduction of CO_2-derived intermediates. Furthermore, Co_5Mn_1PPc maintained a relatively stable current density over 15 h of continuous electrolysis, demonstrating good operational stability. The enhanced performance is potentially associated with electronic and structural interactions between Co and Mn centers within the polyphthalocyanine framework. These findings highlight bimetallic polyphthalocyanines as promising platforms for tuning CO_2RR activity and product selectivity.

Table od content

1. Introduction 1
2. Experimental Methods 3
2.1 Synthesis of MnPPc 3
2.2 Synthesis of Co_5Mn_1PPc 4
2.3 Synthesis of CuPPc 4
3. Sample characterization 5
4. Electrocatalytic CO_2RR measurements H-type cell 5
5. Results and Discussion 6
5.1 Structural Characterization 6
5.1.1 X-ray Diffraction (XRD) 6
5.1.2 Fourier Transform Infrared Spectroscopy (FTIR) 6
5.1.3 Scanning Electron Microscopy (SEM) 6
5.2 Electrochemical Performance 7
5.3 Faradaic Efficiency and Product Selectivity 8
6. Future Work 10
6.1 CuPPc-1 10
6.2 CuPPc-3 10
6.3 characterization of CuPPc 10
7. Conclusion 12
8. References 13

1. Introduction

Carbon dioxide is a greenhouse gas and a major product of fossil fuel combustion, which makes its accumulation a key contributor to climate change. Besides carbon capture and storage, CO_2 can be used as a carbon feedstock to produce value-added fuels and chemicals, helping close the carbon cycle and reduce dependence on fossil resources.[1] Electrochemical CO_2 reduction reaction (CO_2RR) is particularly attractive because it can operate under mild conditions, use renewable electricity, and provide tunable product selectivity through catalyst and electrolyte design.[2] CO_2 can produce products depending on the number of electrons and protons involved. Such as CO and formate, as well as more highly reduced products including methanol, methane, ethylene, and other hydrocarbons and alcohols.

However, CO_2RR is still challenging because CO_2 is a highly stable molecule and require energy to become activated. This can lead to high overpotentials and slow reaction kinetics. In aqueous electrolytes, the hydrogen evolution reaction (HER) is another major challenge, as it competes with CO_2RR for both electrons and active sites.[3] In addition multiple reaction pathways and shared intermediates make product selectivity difficult to control as changes in the catalysts environment can strongly influence the reaction pathway and final products. These challenges highlight the importance of developing catalysts with defined and tunable active sites that can facilitate carbon dioxide activation while controlling reaction pathways and suppressing the HER.[4]

Metal phthalocyanines have attracted interest as molecular electrocatalysts for carbon dioxide reduction due to their well-defined structure and tunable electronic properties. In these molecules, the metal center is coordinated by four nitrogen atoms within the highly conjugated phthalocyanine macrocycle, creating a well-defined metal–N_4 active site.[5] The nature of the central metal can influence CO_2 adsorption, the stabilization of reaction intermediates, and the product selectivity. Different metal centers can therefore lead to significant differences in CO_2RR activity and product formation.[6] For example NiPc and CoPc have demonstrated carbon dioxide reduction activity, particularly when immobilized on carbon supports or incorporated into polymeric structures.[5,7]

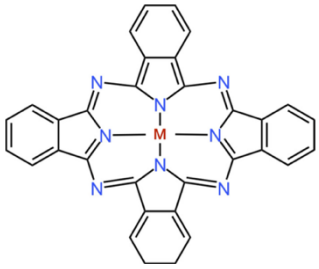


Figure 1. General molecular structure of a metal phthalocyanine (MPc), where M represents the central metal ion coordinated by four nitrogen atoms (M-N_4).

The development of polyphthalocyanine (MPPc) materials from molecular metal phthalocyanines (MPcs) provides another approach to improving the properties of phthalocyanine-based catalysts. In MPPcs, the phthalocyanine units are covalently linked to form an extended π-conjugated framework, which can promote electron transport through the material and create a different

electronic environment around the metal centers.[6] The polymeric structure can also provide greater stability than isolated molecular phthalocyanines.[5,6] However, forming a polymer does not necessarily result in higher CO_2RR activity or Faradaic efficiency. The catalytic behavior still depends strongly on the coordination environment and electronic structure of the metal sites. Therefore, MPPcs offer an opportunity to study how polymer structure and the local environment of the metal centers affect CO_2RR activity and product selectivity.[5,8]

Introducing two metal centers into a polyphthalocyanine framework offers a promising strategy for tuning carbon dioxide reduction activity and selectivity through synergistic effects. Electronic interactions between neighboring metal sites can modify the electron density and the binding strength of key reaction intermediates while different metals may provide complementary catalytic functions. For example bimetallic Co/Zn polyphthalocyanines have demonstrated CO_2 to CO performance compared with their corresponding monometallic systems, highlighting the potential of bimetallic polyphthalocyanine frameworks as a versatile platform for developing more efficient CO_2 reduction catalysts.[8]

Manganese (Mn) is an interesting metal for incorporation into polyphthalocyanine frameworks because of its accessible redox chemistry and ability to exist in several oxidation states, including Mn(I), Mn(II), and Mn(III). which can facilitate electron transfer and stabilization of reaction intermediates during CO_2 reduction.[9] Molecular Mn catalysts, particularly those based on bipyridyl and related ligands, have demonstrated CO_2 to CO activity, highlighting the ability of Mn centers to participate in CO_2 activation and reduction chemistry.[9,10] However, the behavior of these molecular Mn catalysts cannot be directly applied to Mn phthalocyanines or polyphthalocyanines because their coordination environments and extended π-conjugated structures are considerably different.[6,9] Compared with Co, Fe, and Ni-based phthalocyanines, Mn containing phthalocyanine systems have received less attention for CO_2RR. Incorporating Mn into a polyphthalocyanine framework could therefore provide a different redox and electronic environment and may also influence the behavior of neighboring metal sites. Based on this idea, this work first investigates MnPPc to understand its structural, electrochemical, and catalytic properties as a Mn centered polyphthalocyanine. Co_5Mn_1PPc is then studied to examine whether combining Mn with Co can create interactions between the two metal centers and improve or modify CO_2RR performance compared with the corresponding monometallic systems.

Copper polyphthalocyanine (CuPPc) is also proposed as a promising direction for future investigation. Copper based phthalocyanine materials are particularly relevant to CO_2RR because Cu can promote the formation of reduced carbon products, while the molecular structure, crystallinity, and dynamic reconstruction of CuPc derived catalysts under electrochemical conditions can strongly influence the nature of the active sites and product distribution.[11,12,13] In particular, operando studies have shown that CuPc can undergo reversible restructuring under CO_2RR conditions to generate Cu clusters, indicating that the catalytically active state may differ from the initial molecular Cu-N_4 configuration.[11] Extending CuPc into a polyphthalocyanine framework may provide a means of modifying charge transport, metal-site proximity, catalyst robustness, and the restructuring behavior of Cu species during operation.[14] Therefore, further systematic investigation of CuPPc is warranted to establish its structure activity relationship, operational stability, and selectivity toward CO_2RR products, particularly CO, methane, and multicarbon products.

2. Experimental Methods

2.1 Synthesis of MnPPc

MnPPc was synthesized by a solid-phase synthesis method in a muffle furnace. Briefly, a mixture of $MnCl_2 \cdot 4H_2O$ (0.99 g), urea (4.10 g), NH_4Cl (1.00 g), $(NH_4)_6Mo_7O_{24} \cdot 4H_2O$ (0.025 g), phthalic anhydride (0.30 g), and pyromellitic dianhydride (PMDA) (1.74 g) was thoroughly ground into a homogeneous powder. The resulting mixture was placed in a crucible and heated in a muffle furnace at 220 °C for 3 h with a ramp rate of 5 °C min^{-1}. After cooling to room temperature, the obtained product was washed with water, ethanol, and DMF using centrifugation. The washed product was finally dried under vacuum at 80 °C.[15]

For catalyst ink preparation, 7.5 mg of the obtained MnPPc catalyst was dispersed in 15 mL of N-methyl-2-pyrrolidone (NMP), corresponding to a catalyst concentration of 0.5 mg mL^{-1}. The suspension was sonicated for 1 h to obtain a homogeneous catalyst ink.

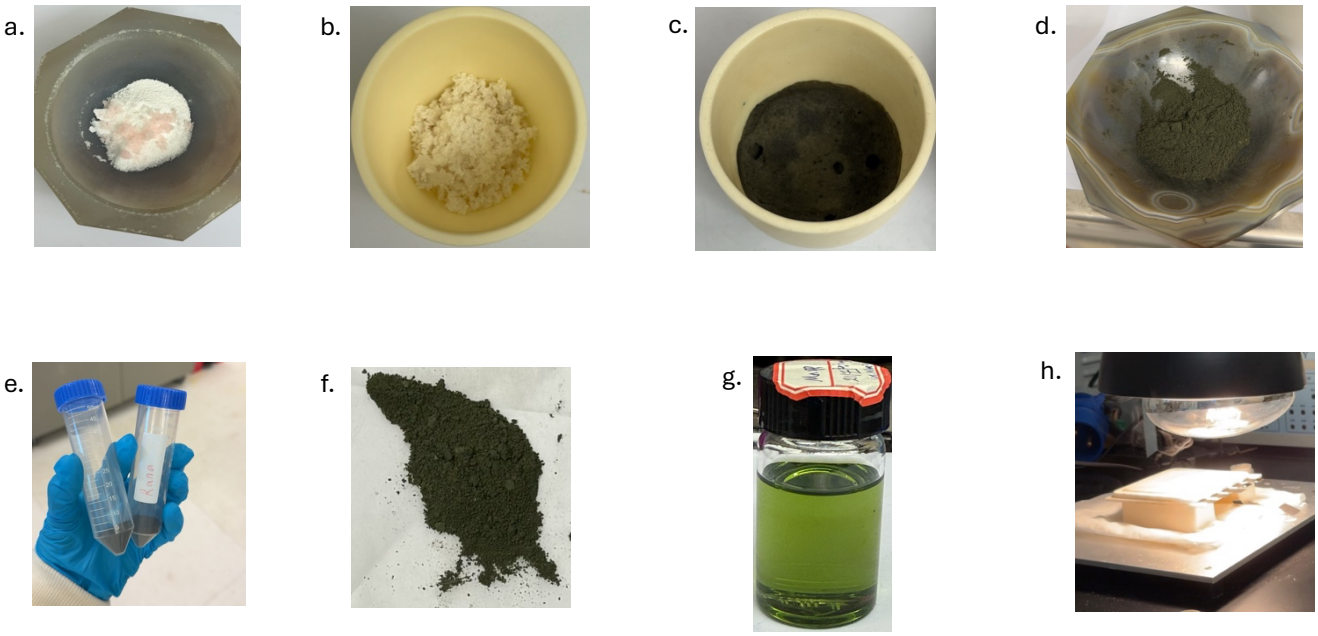


Figure 2. Photographs illustrating the preparation of the MnPPc catalyst and catalyst ink: (a) starting reactants before grinding. (b) homogenized precursor mixture after grinding and transfer into a crucible. (c) precursor powder after thermal treatment in a furnace. (d) furnace treated product after collection and grinding. (e) washing of the product in centrifuge tubes. (f) dried MnPPc powder after vacuum drying and final grinding. (g) homogeneous MnPPc catalyst ink after sonication in (NMP).(h) drop casting of the catalyst ink onto the electrode substrate.

2.2 Synthesis of Co_5Mn_1PPc

Co_5Mn_2PPc was prepared by the same method used for MnPPc, except that $MnCl_2 \cdot 4H_2O$ was replaced with a mixture of $CoCl_2$ and $CoCl_2 \cdot 4\ H_2O$. Briefly,(n $CoCl_2 \cdot 6H_2O$ + n$MCl_2 \cdot 4H_2O$ = 5.00 mmol): $CoCl_2$ (0.54 g, 4.167 mmol) and $MnCl_2 \cdot 4H_2O$ (0.16 g, 0.833 mmol) were used as the metal precursors for Co_5Mn_2PPc.

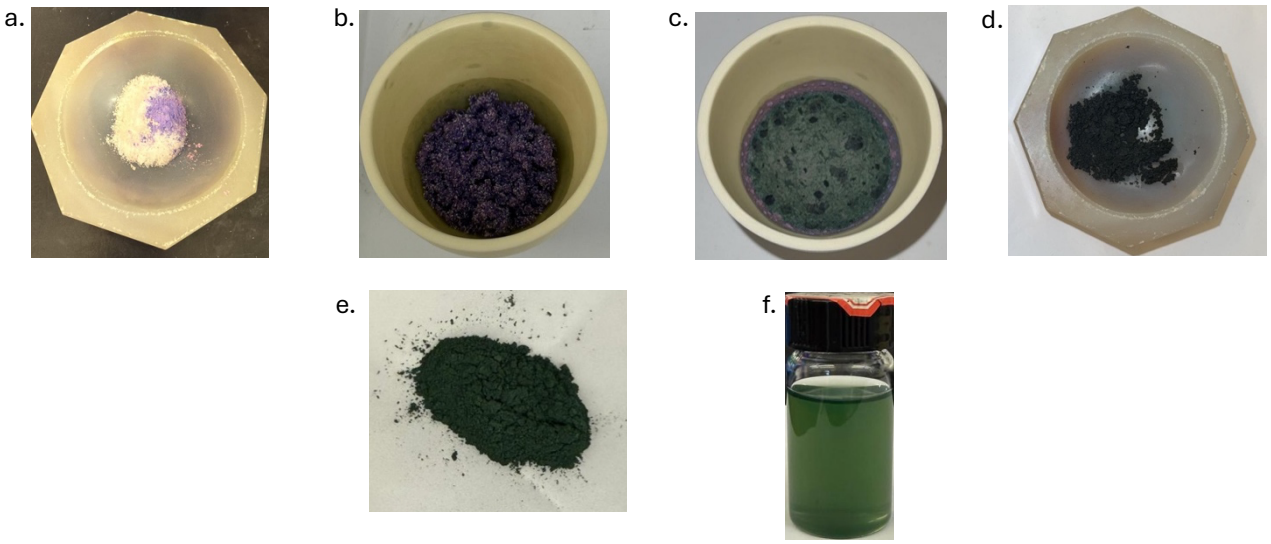
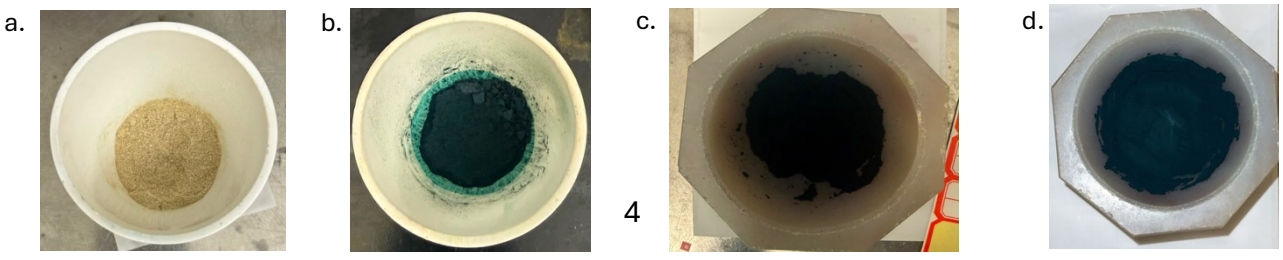


Figure 3. Photographs illustrating the synthesis and catalyst ink preparation of Co_5Mn_1PPc. (a) Metal and organic precursor materials before mixing. (b) Homogeneous precursor mixture after grinding. (c) Product immediately after thermal treatment in the furnace. (d) Heat treated product after collection and grinding. (e) CoMnPPc powder after washing, vacuum drying, and final grinding. (f) Homogeneous CoMnPPc catalyst ink after sonication in (NMP).

2.3 Synthesis of CuPPc

CuPPc was prepared by the same method used for MnPPc, except that $MnCl_2 \cdot 4H_2O$ was replaced with anhydrous $CuCl_2$. Briefly, $CuCl_2$ (0.67 g, 4.98 mmol) was used as the metal precursor for CuPPc. The obtained CuPPc catalyst was used to prepare three catalyst inks under different solvent and sonication conditions. CuPPc-1 was prepared by dispersing 7.5 mg of CuPPc in 15 mL of NMP, followed by sonication for 1 h. CuPPc-2 was prepared by dispersing 7.5 mg of CuPPc in a mixture of 15 mL of NMP and 5 mL of ethanol, followed by sonication for 3 h. CuPPc-3 was prepared by dispersing 3.75 mg of CuPPc in 15 mL of DMF, followed by sonication for 3 h.



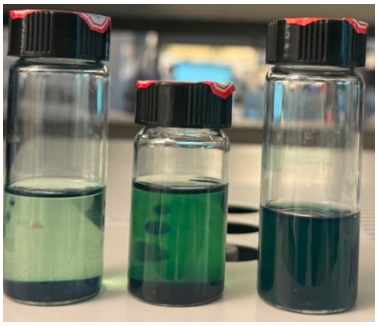
e. 

Figure 4. Photographs illustrating the synthesis and catalyst ink preparation of CuPPc materials. (a) Starting precursor materials (b) Product after thermal treatment. (c) Ground heat treated product. (d) CuPPc powder after centrifugation based washing, vacuum drying, and final grinding. (e) Catalyst inks of CuPPc-2, CuPPc-1, and CuPPc-3, shown from left to right after sonication.

3. Sample characterization

Scanning electron microscopy (SEM) images were obtained to investigate the morphology and surface characteristics of the synthesized MnPPc and Co_5Mn_1PPc samples. Powder X-ray diffraction (XRD) patterns were recorded to investigate the crystalline structure and phase composition of the synthesized materials. Fourier transform infrared (FTIR) spectra were measured to identify the characteristic functional groups and chemical bonding of the synthesized samples and to confirm the formation of the polyphthalocyanine (PPc) structure.

4. Electrocatalytic CO_2RR measurements H-type cell

Electrocatalytic CO_2 reduction reaction (CO_2RR) measurements were conducted in an H-type electrochemical cell. A 0.5 M $KHCO_3$ solution was used as the electrolyte. A carbon paper electrode (2 × 1 cm) was used as the working electrode, with Ag/AgCl and Pt electrodes serving as the reference and counter electrodes, respectively .The working electrode was prepared by drop-casting the catalyst ink onto the carbon paper. First, 80 µL of ethanol was added to the electrode, followed by 400 µL of catalyst ink deposited in five successive 80 µL drops. Subsequently, 50 µL of Nafion solution (diluting 1 mL of Nafion with 4 mL of ethanol) was dropcast onto the electrode.

Before the electrochemical measurements, the cathodic compartment was purged with CO_2 gas for 20 min to obtain CO_2 saturated electrolyte. Chronoamperometric (CA) measurements were performed at different applied potentials ranging from -0.8 to -1.2 V versus RHE, all potentials in the studies were converted to the potential versus RHE according to the equation E (vs RHE) = E (vs Ag/ AgCl) + 0.1989 V + 0.059 × pH. With each measurement conducted for 30 min. CO_2 was supplied at a flow rate of 20 mL min^{-1}. Gas products were analyzed using gas chromatography (GC). The first GC measurement was performed after 10 min of electrolysis, followed by a second measurement after an additional 10 min.

For liquid product analysis, electrolyte samples were collected from the cathodic compartment after electrolysis and analyzed by nuclear magnetic resonance (NMR) spectroscopy. For NMR analysis, 2000 μL of electrolyte was mixed with 200 μL of D_2O and 40 μL of DMSO. The resulting mixture was homogenized, and 560 μL of the prepared solution was transferred into each NMR tube for analysis.

5. Results and Discussion

5.1 Structural Characterization

5.1.1 X-ray Diffraction (XRD)

The XRD patterns of MnPPc and Co_5Mn_1PPc (Fig. 4 a,d) were analyzed to investigate the structural characteristics and crystallinity of the synthesized materials. MnPPc exhibited relatively distinct diffraction peaks along with several additional reflections, indicating a relatively well ordered crystalline structure. In comparison, Co_5Mn_1PPc showed diffraction peaks at similar positions, suggesting that the incorporation of Co did not lead to a significant change in the overall structural framework of MnPPc. However, the diffraction peaks of Co_5Mn_1PPc were less intense and broader, accompanied by a more pronounced background contribution, indicating a decrease in the degree of crystallinity.

This decrease in crystallinity may be associated with the incorporation of a second metal center into the polyphthalocyanine framework, which can introduce local structural disorder and affect the long range ordering of the polymeric network. Nevertheless, the retention of the main diffraction features suggests that the fundamental structure of the Mn-based polyphthalocyanine framework was maintained after the introduction of Co.

5.1.2 Fourier Transform Infrared Spectroscopy (FTIR)

The FTIR spectra of MnPPc and Co_5Mn_1PPc (Fig. 4b,e) show several characteristic bands of the phthalocyanine ring. These characteristic vibrational modes are consistent with the formation of the phthalocyanine framework, supporting the successful synthesis of MnPPc and Co_5Mn_1PPc.

5.1.3 Scanning Electron Microscopy (SEM)

The SEM image of MnPPc (Fig. 4c) shows relatively small, irregular aggregates with needle- or sheet-like features distributed across the surface. In contrast, Co_5Mn_1PPc (Fig.4f) showed larger and more irregular agglomerated structures. This morphological change suggests that the incorporation of Co affected the growth and aggregation behavior of the polyphthalocyanine network during synthesis. The formation of larger aggregates in Co_5Mn_1PPc may influence the accessible surface area and the exposure of catalytically active sites. Therefore, the morphological differences between MnPPc and Co_5Mn_1PPc may contribute to their different electrochemical behaviors.

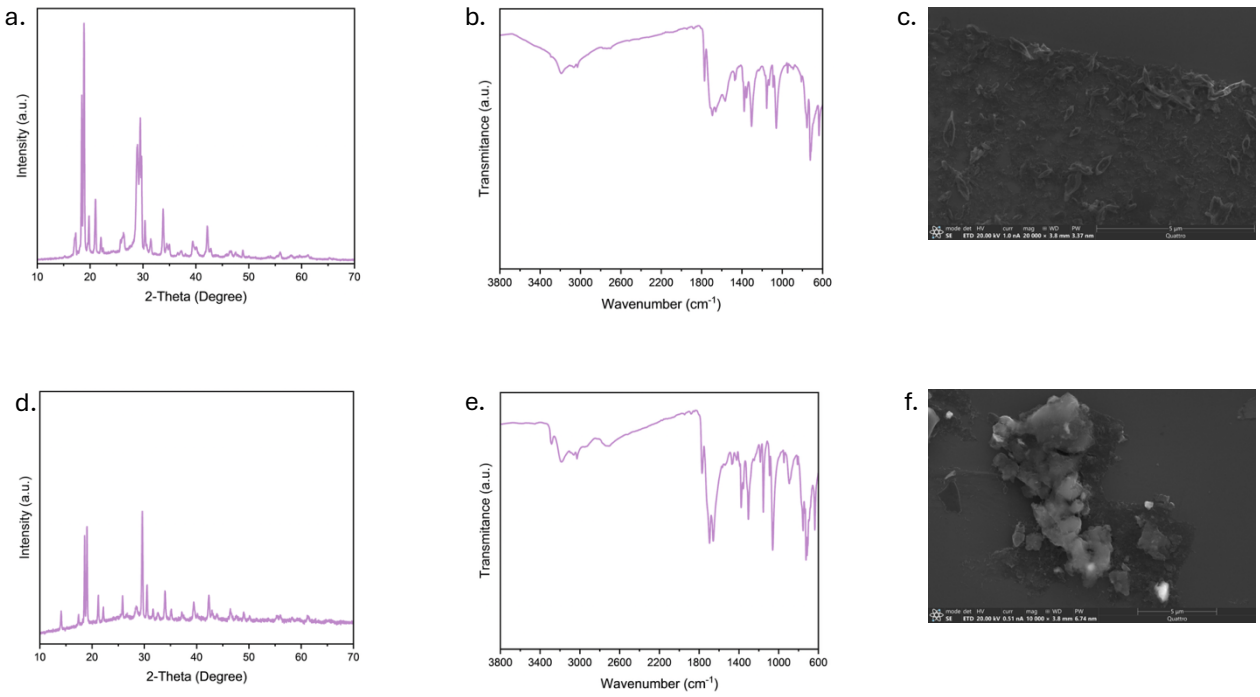


Figure 5. Structural and morphological characterization of MnPPc Co_5Mn_1PPc. (a) XRD pattern of MnPPc. (b) FTIR spectrum of MnPPc. (c) SEM image of MnPPc. (d) XRD pattern of CoMnPPc. (e) FTIR spectrum of CoMnPPc. (f) SEM image of CoMnPPc.

5.2 Electrochemical Performance

Chronoamperometry (CA)

The electrochemical behavior of MnPPc and Co_5Mn_1PPc was evaluated by chronoamperometry at different applied potentials. As shown in (Fig.6 a), MnPPc exhibited relatively low current densities at less negative potentials, ranging from -0.80 to -1.00 V, with current densities generally below -5 mA cm^{-2}. However, when the applied potential was increased to -1.10 and -1.20 V, the current density increased substantially, reaching values as high as approximately -42 mA cm^{-2}. Despite the higher current response, the current profiles at these potentials showed pronounced fluctuations and a significant decrease with time, indicating relatively poor electrochemical stability under these operating conditions. In contrast, Co_5Mn_1PPc exhibited substantially higher current densities over the investigated potential range, reaching approximately -10 to -35 mA cm^{-2} depending on the applied potential (Fig.6 c). Moreover, the current profiles generally reached a relatively stable plateau after the initial transient period, with less pronounced fluctuations compared with MnPPc. These results indicate that the incorporation of Co significantly altered the electrochemical response of the Mn-based catalyst and improved its current stability.

The higher current response of Co_5Mn_1PPc may be related to changes in the electronic environment of the metal centers and the interaction between Co and Mn sites within the polyphthalocyanine framework. In addition, the modified morphology and potentially improved

charge transfer behavior may contribute to the enhanced electrochemical activity. The competition between CO_2 reduction and the hydrogen evolution reaction (HER) may also influence the current response, particularly at more negative potentials.

5.3 Faradaic Efficiency and Product Selectivity

The product distribution of MnPPc and Co_5Mn_1PPc was evaluated by determining the Faradaic efficiency (FE) of the detected gaseous and liquid products.

MnPPc

As shown in (Fig.6 b), H_2 was the dominant product for MnPPc across the investigated potential range, indicating that the catalyst predominantly favored the competing hydrogen evolution reaction. A limited amount of CO was detected at -0.80 to -1.00 V, with FE_{CO} values of approximately 15-28%. However, at the more negative potentials of -1.10 and -1.20 V, CO production was nearly suppressed and H_2 became the dominant product.

These results indicate that MnPPc alone has limited selectivity toward electrochemical CO_2 reduction under the investigated conditions. The increasing contribution of HER at more negative potentials suggests that applying a higher overpotential does not necessarily improve CO_2RR selectivity and instead promotes the competing hydrogen evolution pathway.

Co_5Mn_1PPc

In contrast, Co_5Mn_1PPc demonstrated a substantial improvement in CO_2RR selectivity (Fig.6 d). CO was the dominant product across the investigated potential range, with FE_{CO} values ranging from approximately 70% to above 90%. This represents a significant change in product distribution compared with MnPPc, where H_2 was the major product.

Interestingly, methanol (MeOH) was also detected at the more negative potentials of -1.10 and -1.20 V. The appearance of MeOH suggests that Co_5Mn_1PPc may facilitate further reduction of CO_2 derived intermediates under sufficiently reducing conditions. This behavior is particularly important because it indicates that incorporation of Co not only enhanced CO_2RR selectivity over HER but also altered the product distribution toward a more deeply reduced carbon product.

The improved CO_2RR performance of Co_5Mn_1PPc can potentially be attributed to the synergistic electronic interaction between the Co and Mn centers. The incorporation of a second metal center may modify the electronic structure of the active sites and influence the adsorption and stabilization of CO_2RR intermediates. However, further characterization and mechanistic studies would be required to directly establish the origin of the enhanced selectivity and the formation pathway of methanol.

The long term electrochemical stability of Co_5Mn_1PPc was evaluated at -1.00 V for 15 h (Fig.6 e). The catalyst maintained a relatively stable current density throughout the test, remaining approximately within the range of -22 to -25 mA cm^{-2}, with no significant decline in current over the testing period.

The sustained current response indicates that Co_5Mn_1PPc possesses good electrochemical stability under the investigated operating conditions. The presence of Mn may contribute to the stability of the polyphthalocyanine framework by helping maintain its structural integrity during prolonged electrochemical operation. This stability, together with the relatively high current density and high CO selectivity of Co_5Mn_1PPc, highlights its potential as an electrocatalyst for CO_2 reduction. Further post-electrolysis structural characterization would be valuable to verify the preservation of the catalyst structure after prolonged electrochemical operation.

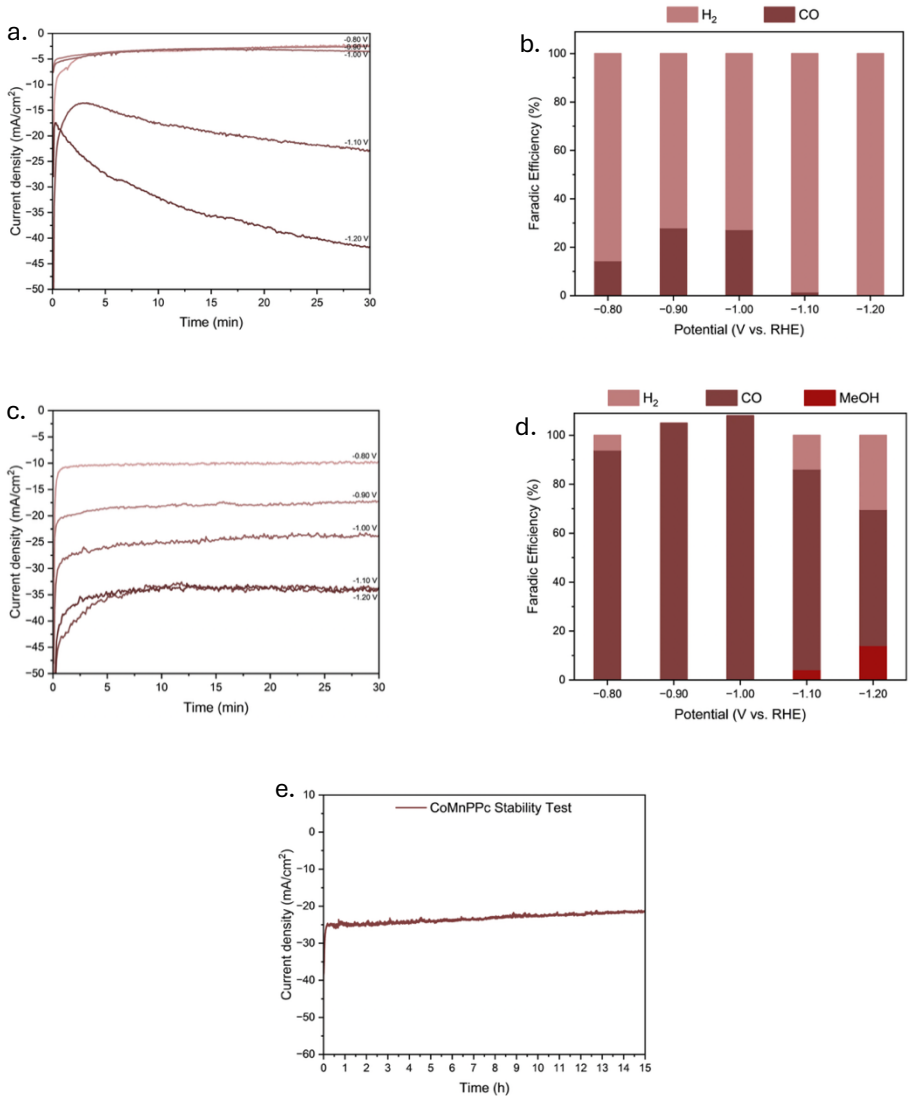


Figure 6. Electrochemical CO_2 reduction performance of MnPPc and Co_5Mn_1PPc. (a) Faradaic efficiencie for MnPPc. (b) Chronoamperometric current density of MnPPc. (c) Faradaic efficiencie for Co_5Mn_1PPc. (d) Chronoamperometric current density of Co_5Mn_1PPc. (e) Long term chronoamperometric stability test of Co_5Mn_1PPc at the selected potential for 15 h.

6. Future Work

To investigate the electrochemical CO_2 reduction performance of CuPPc, chronoamperometric measurements were performed using NMP and DMF as solvents at different applied potentials. The effect of electrochemical pre-reduction was also investigated by applying a more negative potential before performing CA at less negative potentials.

6.1 CuPPc-1

As shown in (Fig. 7a), the current density of CuPPc in NMP increased as the applied potential became more negative. After the initial current response, the current remained relatively stable throughout the CA measurements, indicating good electrochemical stability under the investigated conditions. In (Fig. 7b), H_2 was the dominant product at most potentials. Formate formation became apparent at -1.00 V and reached approximately 26% at -1.10 V, while its FE decreased to approximately 13% at -1.20 V. This indicates that more negative potentials increasingly favored HER rather than formate production. After pre-reduction as shown in (Fig. 7c), CuPPc was first subjected to -1.75 V vs. RHE for 3 min, followed by CA at less negative potentials. Formate was detected at -0.80 V with an FE comparable to that obtained at -1.10 V under direct potential application. CO formation also increased, particularly at -1.00 and -1.20 V. These changes suggest that the pre-reduction step modified the Cu surface and affected the product distribution. However, H_2 remained a major product, indicating that HER was still significant.

6.2 CuPPc-3

in (Fig. 7d), H_2 remained the dominant product in DMF. However, formate appeared at -0.90 V and reached approximately 23% at -1.00 V, accompanied by a FE_{CO} of approximately 16%. Compared with NMP, DMF therefore showed an earlier onset of formate formation and higher CO production under direct potential application. CuPPc after pre-reduction as shown in (Fig. 7e), CuPPc was subjected to -1.50 V vs. RHE for 7 min before CA. Unlike NMP the pretreatment did not result in a clear improvement in CO_2 derived product formation. H_2 remained dominant, particularly at -0.80 V, while formate and CO were observed at more negative potentials. The difference may be related to the different pretreatment potentials and durations used for NMP and DMF.

6.3 characterization of CuPPc

The SEM images show a clear morphological difference in CuPPc before and after the reaction. Before the reaction (Fig.8a), CuPPc exhibited an irregular, rough, and highly agglomerated morphology with no clearly distinguishable Cu nanoparticles. After the reaction (Fig. 8b), numerous fine nanoscale particles appeared on the CuPPc surface, indicating the formation of Cu nanoparticles during the electrochemical reaction. Their elemental composition can be further confirmed by EDS analysis.

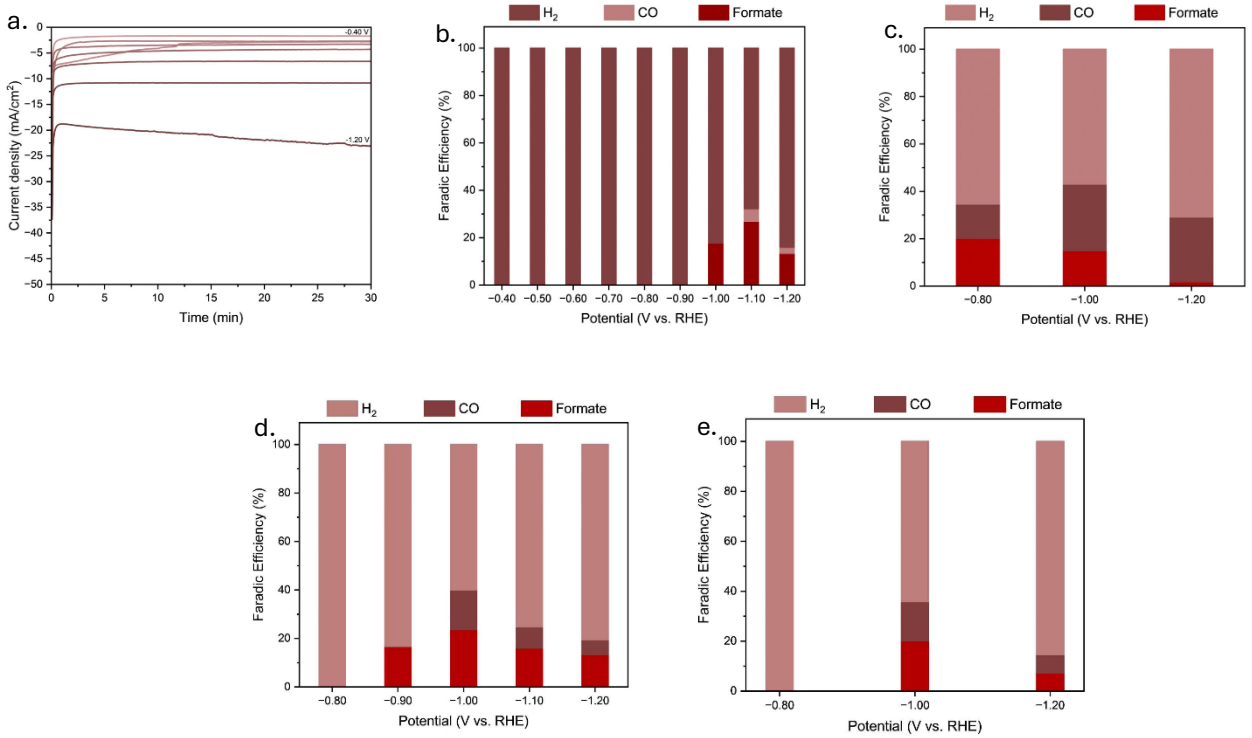


Figure 7. Electrochemical CO_2 reduction performance of CuPPc in NMP and DMF. (a) Chronoamperometric current density of CuPPc in NMP at different potentials. (b) Faradaic efficiency of CuPPc in NMP under direct potential application. (c) Faradaic efficiency after pre-reduction at -1.75 V vs. RHE, followed by CA at less negative potentials. (d) Faradaic efficiency of CuPPc in DMF under direct potential application. (e) Faradaic efficiency after pre-reduction at -1.50 V vs. RHE, followed by CA at less negative potentials.

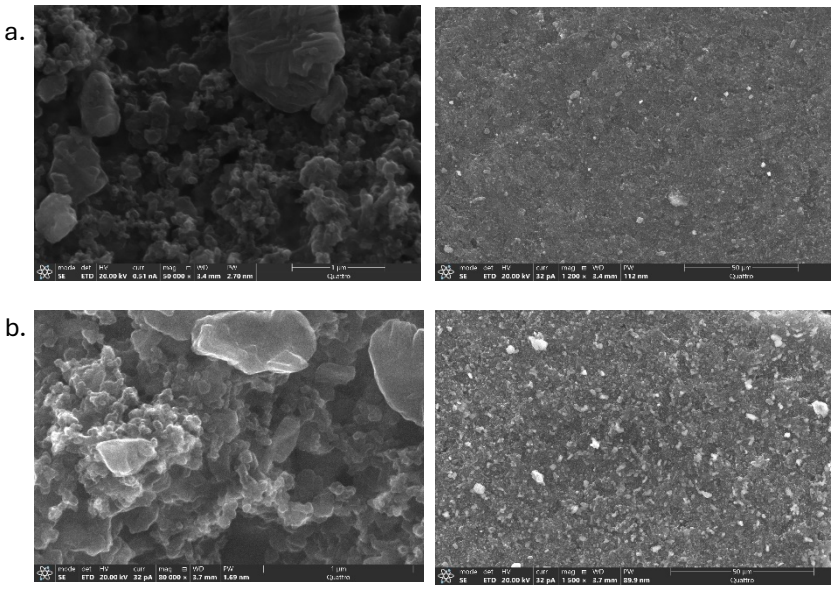


Figure 8. SEM images of CuPPc before and after the reaction at different magnifications (a) Before the reaction. (B) After the reaction.

Future work will focus on further investigating CuPPc for electrochemical CO_2 reduction by optimizing the pre-reduction conditions in NMP and DMF. EDX, TEM and XPS characterization will be used to investigate changes in the Cu morphology and surface state after electrochemical treatment. Further optimization of the applied potentials will also be performed to improve formate and CO production while minimizing HER.

7. Conclusion

In this work, MnPPc and bimetallic Co_5Mn_1PPc polyphthalocyanines were successfully synthesized and investigated as electrocatalysts for electrochemical CO_2 reduction. Structural characterization using XRD, FTIR, and SEM confirmed the formation of polyphthalocyanine based materials and revealed differences in crystallinity and morphology following the incorporation of Co. Electrochemical results demonstrated a clear difference between the monometallic and bimetallic catalysts. MnPPc predominantly favored the hydrogen evolution reaction, resulting in limited CO_2RR selectivity. In contrast, Co_5Mn_1PPc exhibited higher and more stable current densities together with substantially improved CO selectivity, reaching FE_{CO} values of up to above 90% under the investigated conditions. Methanol was also detected at more negative potentials, suggesting that the bimetallic system may facilitate further reduction of CO_2 derived intermediates. In addition, Co_5Mn_1PPc maintained a relatively stable current response during 15 h of continuous electrolysis, indicating good operational stability. Overall, the results suggest that incorporating Co into the MnPPc framework can significantly modify the electrochemical behavior and product selectivity, potentially through interactions between the two metal centers and changes in the local electronic and structural environment. Further work involving post electrolysis characterization and mechanistic studies is needed to clarify the active sites and confirm the origin of the enhanced CO_2RR performance and methanol formation.

8. References

1. Wang, C., Zhang, Y., Zhao, F., Zhao, D., & Zhang, J. (2025). Design principles of metal phthalocyanine for electrochemical CO_2 reduction: From targeted molecular structures to atomic-level active sites. *Small, 21*(25), e2502897. https://doi.org/10.1002/smll.202502897
2. Garg, S., Li, M., Weber, A. Z., Ge, L., Li, L., Rudolph, V., Wang, G., & Rufford, T. E. (2020). Advances and challenges in electrochemical CO_2 reduction processes: An engineering and design perspective looking beyond new catalyst materials. *Journal of Materials Chemistry A, 8*(4), 1511–1544. https://doi.org/10.1039/C9TA13298H
3. Jin, S., Hao, Z., Zhang, K., Yan, Z., & Chen, J. (2021). Advances and challenges for the electrochemical reduction of CO_2 to CO: From fundamentals to industrialization. *Angewandte Chemie International Edition, 60*(38), 20627–20648. https://doi.org/10.1002/anie.202101818
4. Allangawi, A., Xiao, X. T., Ma, X., Alsuhami, M., Khan, M. A., Aleisa, R., Kobayashi, Y., Li, W.-L., Rueping, M., Gascon, J., & Zhang, H. (2025). Selective electrocatalytic CO_2 reduction to methanol: A roadmap toward practical implementation. *Angewandte Chemie International Edition, 64*(52), e202517916. https://doi.org/10.1002/anie.202517916
5. Liu, Y., & McCrory, C. C. L. (2019). Modulating the mechanism of electrocatalytic CO_2 reduction by cobalt phthalocyanine through polymer coordination and encapsulation. *Nature Communications, 10*, 1683. https://doi.org/10.1038/s41467-019-09626-8
6. Chang, Q., Liu, Y., Lee, J.-H., Ologunagba, D., Hwang, S., Xie, Z., Kattel, S., Lee, J. H., & Chen, J. G. (2022). Metal-coordinated phthalocyanines as platform molecules for understanding isolated metal sites in the electrochemical reduction of CO_2. *Journal of the American Chemical Society, 144*(35), 16131–16138. https://doi.org/10.1021/jacs.2c06953
7. Wu, Y., Jiang, Z., Lu, X., Liang, Y., & Wang, H. (2019). Domino electroreduction of CO_2 to methanol on a molecular catalyst. *Nature, 575*(7784), 639–642. https://doi.org/10.1038/s41586-019-1760-8
8. Li, N., Si, D.-H., Wu, Q.-J., Wu, Q., Huang, Y.-B., & Cao, R. (2023). Boosting electrocatalytic CO_2 reduction with conjugated bimetallic Co/Zn polyphthalocyanine frameworks. *CCS Chemistry, 5*(5), 1130–1143. https://doi.org/10.31635/ccschem.022.202201943
9. Siritanaratkul, B., Eagle, C., & Cowan, A. J. (2022). Manganese carbonyl complexes as selective electrocatalysts for CO_2 reduction in water and organic solvents. *Accounts of Chemical Research, 55*(7), 955–965. https://doi.org/10.1021/acs.accounts.1c00692
10. Sampson, M. D., Nguyen, A. D., Grice, K. A., Moore, C. E., Rheingold, A. L., & Kubiak, C. P. (2014). Manganese catalysts with bulky bipyridine ligands for the electrocatalytic reduction of carbon dioxide: Eliminating dimerization and altering catalysis. *Journal of the American Chemical Society, 136*(14), 5460–5471. https://doi.org/10.1021/ja501252f
11. Weng, Z., Wu, Y., Wang, M., Jiang, J., Yang, K., Huo, S., Wang, X.-F., Ma, Q., Brudvig, G. W., Batista, V. S., Liang, Y., Feng, Z., & Wang, H. (2018). Active sites of copper-complex catalytic materials for electrochemical carbon dioxide reduction. *Nature Communications, 9*, 415. https://doi.org/10.1038/s41467-018-02819-7
12. Kusama, S., Saito, T., Hashiba, H., Sakai, A., & Yotsuhashi, S. (2017). Crystalline copper(II) phthalocyanine catalysts for electrochemical reduction of carbon dioxide in aqueous media. *ACS Catalysis, 7*(12), 8382–8385. https://doi.org/10.1021/acscatal.7b02220
13. Zhang, J., Pham, T. H. M., Gao, Z., Li, M., Ko, Y. H., Lombardo, L., Zhao, W., Luo, W., & Züttel, A. (2023). Electrochemical CO_2 reduction over copper phthalocyanine derived catalysts with enhanced selectivity for multicarbon products. *ACS Catalysis, 13*(14), 9326–9335. https://doi.org/10.1021/acscatal.3c01439
14. Karapinar, D., Zitolo, A., Huan, T. N., Zanna, S., Taverna, D., Tizei, L. H. G., Giaume, D., Marcus, P., Mougel, V., & Fontecave, M. (2020). Carbon-nanotube-supported copper polyphthalocyanine for efficient and selective electrocatalytic CO_2 reduction to CO. *ChemSusChem, 13*(1), 173–179. https://doi.org/10.1002/cssc.201902859
15. Yang, S., Yu, Y., Dou, M., Zhang, Z., & Wang, F. (2020). Edge-functionalized polyphthalocyanine networks with high oxygen reduction reaction activity. *Journal of the American Chemical Society, 142*(41), 17524–17530. https://doi.org/10.1021/jacs.0c07249